

Simultaneous Removal of Multipollutants (VOCs/NO/SO₂) by Catalytic Ozonation Coupled with Wet Scrubbing Technology: From the Laboratory to Industrial Testing

Peixi Liu, Yiwei Zhang, Xiaojun Ma, Chaoqun Xu, Yong He, Yanqun Zhu, Elisabete C. B. A. Alegria, Zhihua Wang,* and Armando J. L. Pombeiro



Cite This: *Ind. Eng. Chem. Res.* 2024, 63, 8610–8621



Read Online

ACCESS |

Metrics & More

Article Recommendations

Supporting Information

ABSTRACT: The simultaneous removal of multi-VOCs (C₃H₆O/C₆H₆/C₇H₈/C₈H₁₀) and NO/SO₂ by catalytic ozonation on the CoO_x-CrO_x/γ-Al₂O₃ (SCC) catalyst was studied on a laboratory scale and in industrial field testing, respectively. It was discovered that the removal efficiencies of aromatic VOCs gradually increased as the excess ozone ratio (λ), the ratio of the actual number of moles of ozone to the theoretical number, increased. With the help of a wet scrubbing system, multi-VOCs and SO₂ can be completely removed. The removal efficiency of NO remained above 95%, and the NO₂ selectivity was only 2%. The applicability of the SCC catalyst at lower temperatures was verified by achieving conversion efficiencies of multiple pollutants of more than 80% at 50 °C, with the scrubbing system. In an industrial field-scale test performed in a textile mill in Anhui Province, China, it was proven that in the absence of catalyst assistance, VOCs with high molecular weight were gradually degraded and small molecules such as methanol, formaldehyde, and formic acid were generated more. Coupled with the SCC catalyst, at $\lambda = 3$, the concentrations of almost all major VOC pollutants could be degraded to <3 ppm. Analyzed by XRD, O₂-TPD, H₂-TPR, XPS, and ICP-OES characterizations, the excellent activity and stability of the SCC catalysts are attributed to the good dispersion of metal oxides, strong intermetallic interactions, excellent reducibility, rapid redox cycles of Cr³⁺/Cr⁶⁺ and Co²⁺/Co³⁺, and abundant chemisorbed oxygen. The slight deactivation of the SCC catalysts utilized continuously in the textile mill may be related to the loss of active Cr⁶⁺ and Co²⁺. The results show that the combination of catalytic ozonation technology and the wet scrubbing system can realize the efficient and simultaneous removal of multiple pollutants, providing an experimental and practical basis for further industrial application.



1. INTRODUCTION

Due to rapid industrialization in many countries, such as China, substantial quantities of various air pollutants, including NO_x, SO₂, and volatile organic compounds (VOCs), are emitted from industries such as power plants, steel production, and building materials.¹ VOCs, characterized by boiling points ranging from 50 to 260 °C, are recognized as precursors of PM 2.5 and O₃, contributing to the formation of secondary photochemical smog and organic aerosols in the atmosphere.² These pollutants interact with each other, causing serious environmental problems, such as haze, photochemical smog, acid rain, etc., threatening human health and environmental ecology.³ Under stricter regulations of pollutant emission by the Chinese government in recent years, breakthroughs in NO_x and SO₂ control technologies have been made in major industrial sectors.⁴ Following the effective control of NO_x, SO₂, and other conventional pollutants, VOCs have attracted a lot of attention in recent years.¹ The emission control of VOCs in China started late. The national emission standard “Integrated emission standard of air pollutants” (GB 16297-1996) stipulated the maximum emission concentration limit and

emission rate of benzene, toluene, xylene, phenols, and other VOCs. The Air Pollution Prevention and Control Law of the People’s Republic of China (2015) for the first time included emission control of VOCs in the scope of legal supervision. During the “12th Five-Year Plan” period, China has successively formulated a series of national emission standards and put forward stricter requirements for VOC emission control in key industries, including the rubber products industry pollutant emission standard (GB 27632-2011), steel rolling industry air pollutant emission standard (GB 28665-2012), petroleum refining industry emission standard (GB 31570-2015), petrochemical industry emission standard (GB 31571-2015). During the “13th Five-Year Plan” period, the

Received: February 22, 2024

Revised: April 19, 2024

Accepted: April 24, 2024

Published: April 30, 2024



“13th Five-Year Plan” Work Plan for VOCs Pollution Prevention and Control issued by the Ministry of Environmental Protection in 2017 put forward the main goals for VOC emission reduction: By 2020, total emissions will be decreased by more than 10% compared with 2015. The Chinese government has set more rigorous targets, aiming to reduce VOC emissions by at least 10% compared with 2020 levels by the year 2025.² In the new released plan, the air pollution evaluation index was revised from “SO₂ and NO_x” to “VOC and NO_x”.² However, the removal of VOCs becomes more difficult due to the wide variety, with various physical and chemical properties.⁵

Traditional methods of pollutant removal usually contain a series of individual processes, such as selective catalytic reduction (SCR) and selective noncatalytic reduction (SNCR) for NO_x abatement, flue gas desulfurization for SO₂ removal, needing an amount of capital investment, more space, and more complex systems and processes, respectively.^{2,6} Simple combinations always lead to an increase in capital and operating costs.³ However, for the existing flue gas purification technology, a feasible method for SCR reactors to remove multiple pollutants simultaneously has not been identified.² The complex interactions among various pollutants also make it knotty.^{2,5} Besides, due to inappropriate temperature ranges and complex flue gas compositions, these technical routes are usually not easily utilized in many industries.³ Therefore, further investigation and exploration of integrated technology in the simultaneous and efficient removal of VOCs and conventional pollutants, i.e., NO_x, SO₂, and PM, are more attractive to meet the requirements of ultralow emissions standards and good economic performance,⁶ especially based on the existing air pollution control devices.^{1,2}

Catalytic oxidation technology is widely considered to be one of the most promising strategies for eliminating VOCs,² with harmless CO₂ and H₂O as final products with relatively low temperatures. For NO_x removal, besides SCR/SNCR technologies, oxidation technology for the removal of NO_x is also attractive through the oxidation of low-solubility NO, which accounts for at least 95% of NO_x in typical combustion flue gas,^{6,7} into more soluble NO₂ or N₂O₅. For SO₂ removal, wet flue gas desulfurization (WFGD) technologies are widely used for their simple operation, low cost, and good performance. Catalytic ozonation, one of the promising technologies, utilizes the stronger oxidation ability of ozone and catalysts, which can oxidize both NO and VOCs under low temperatures.^{3,5,8,9} Catalytic ozonation technology can also assist the typical WFGD system in simultaneously removing NO_x, SO₂, and VOC pollutants.³

The noble metal oxide catalysts exhibit remarkable catalytic activities and stabilities; however, their higher cost and susceptibility to catalyst poisoning caused by SO₂ and moisture in the flue gas present challenges.^{2,10} As a more cost-effective alternative, first-row transition-metal oxide catalysts are considered optimal for catalyzing the oxidation of VOCs due to their reasonable price, high catalytic activity, selectivity, and strong resistance to toxicity.² The application of single or a combination of transition-metal oxide catalysts for VOC degradation has been widely reported.^{2,5,8,9,11} However, the worse chemical and thermal stabilities of single metal oxides can result in particle clustering, leading to a decrease in catalytic performance.^{2,12} To address this issue, bimetallic or multiple transition-metal oxide catalysts have been explored to enhance thermal stability, adjust the electronic structure, and

modify surface properties,² which are more flexible due to the diversity of the active components.¹³ The introduction of secondary metal oxides can effectively reduce the crystallinity and produce intermetallic synergies, generating more oxygen vacancies, to improve the catalytic activity.² It is reported that CrO_x catalysts perform effectively in VOC removal under low temperatures,^{5,9,13} especially with a Cr content of 1.5%. CoO_x-based catalysts have also obtained wide attention in VOC catalytic oxidation, of which the high activity is related to its mobile oxygen species and high oxygen-binding rate,² with Co content of 2.5%. Additionally, a catalyst support with a high specific surface area and porous characteristics can improve the mass-transfer efficiency and adsorption capacity of VOCs.² According to the work reported,^{8,14,15} the catalysts supported by γ -Al₂O₃ have better activity than those supported by TiO₂ or SiO₂ for catalytic ozonation by VOCs. Therefore, Co2.5%-Cr1.5%/ γ -Al₂O₃ catalysts were prepared in this article for the simultaneous and efficient removal of multiple pollutants, including multi-VOCs, NO_x, and SO₂.

Due to the small scales and dispersed distributions, most industrial boilers and furnaces have not yet completed ultralow emission retrofit, becoming the main emission source.³ The field testing and research of multiple pollutant removal in realistic industries is even less studied. The catalytic ozonation technology for the degradation of VOCs can be coupled with ozone deNO_x technology, combined with the existing scrubbing tower in the plant to absorb the oxidation products, with less transformation difficulty, basically no pressure loss, and less change in the flue gas channel, so that it can be applied to most of the industrial boilers of various types, such as chain furnaces, carbon black drying furnaces, and fluidized bed boilers. It is also suitable for the removal of a variety of VOCs, including benzene, toluene, xylene, chlorobenzene, formaldehyde, acetone, dichloromethane, dichloroethane, vinyl chloride, and PCDD/FS.

This article addresses the gap by presenting research on the simultaneous removal of multipollutants (VOCs/NO/SO₂) through catalytic ozonation technology, in both the laboratory and in industrial on-site testing. The findings provide a feasible integrated system for the comprehensive treatment of multiple pollutants in industrial application.

2. EXPERIMENTAL SECTION

2.1. Catalyst Preparation. The spherical CoO_x-CrO_x/ γ -Al₂O₃ (SCC) catalyst was prepared using a two-step isovolumic impregnation method, involving active spherical γ -Al₂O₃ as the support and the sequential loading of CrO_x and CoO_x. The preparation steps were as follows: (1) The active spherical γ -Al₂O₃ with a diameter of 3–5 mm underwent pretreatment by calcination at 600 °C for 2 h. (2) 1.1 mL of Cr(NO₃)₃ solution with a concentration of 104.934 g/L was added dropwise and evenly onto 1 g of a calcinated spherical γ -Al₂O₃ support and then under ultrasonication for 1 h and settlement for 23 h. (3) The liquid–solid mixture was then put in the oven and dried at 100 °C for 7 h, followed by calcination at 500 °C for 4 h, to obtain the Cr1.5%/ γ -Al₂O₃ catalyst, recorded as Cr1.5%. (4) 1 g of Cr1.5% was used as the support of the secondary impregnation, and 1.1 mL of Co(NO₃)₂ solution (concentration 112.107 g/L) was uniformly dropped into the Cr1.5% support. As for Cr1.5% before, Co2.5%-Cr1.5%/ γ -Al₂O₃ was obtained after calcination at 500 °C for 4 h, written as the SCC catalyst. In the preparation process, the

calcination heating rate was 2 °C/min, and the prepared catalysts were spherical with 3–5 mm diameter.

2.2. Catalyst Characterization. X-ray powder diffraction (XRD) patterns of catalysts were obtained from an X-ray diffractometer (X-pert powder, PANalytical B.V.) at 40 kV and 40 mA with Cu K α radiation ($\lambda = 0.1540598$ nm), and the radiation range was 10–80° (2θ , diffraction angle). The actual loadings of Co and Cr elements on the SCC catalysts before and after application were determined by inductively coupled plasma optical emission spectroscopy (ICP-OES). The 50 mg of SCC catalyst was finely ground, digested by an 8 mL digestion solution prepared with the volume ratio of HCl:HNO₃ = 1:3, and then diluted to a 500 mL solution for ICP-OES characterization. The measurements of O₂ temperature-programmed desorption (O₂-TPD) and H₂ temperature-programmed reduction (H₂-TPR) were conducted with an automatic temperature-programmed chemisorption analyzer (AutoChem II 2920, Micromeritics). XPS spectra of the SCC catalysts were collected by an X-ray photoelectron spectrometer (ESCALAB 250Xi, Thermo Scientific), which was equipped with a standard Al K α (1486.6 eV) source, with all binding energies calibrated with the C 1s peak (284.8 eV) as a reference.

2.3. Catalyst Activity Evaluation on the Laboratory Scale. The schematic diagram of the laboratory-scale catalyst activity evaluation system is shown in Figure S1, comprising a gas supply system, reaction system and measurement system. The simulated exhaust gas was mainly composed of five kinds of gases, all of which are cylinder gases (Jingong Gas Co., Ltd.), including N₂ (99.999%), O₂ (99.999%), NO (2000 ppm/balance N₂), SO₂ (1000 ppm/balance N₂), and multi-VOCs (10 ppm acetone/30 ppm benzene/30 ppm toluene/30 ppm *o*-xylene/balance N₂), with a simulated flue gas flow rate of 1 or 4 L/min. Initial concentrations of NO and SO₂ were 100 and 200 ppm, respectively. The initial concentrations of various VOCs were configured to be 5 ppm acetone, 15 ppm benzene, 15 ppm toluene, and 15 ppm *o*-xylene. The O₂ gas entered a dielectric barrier discharge ozone generator (VMUS-1S type, 1 g, Canada AZCO) to generate ozone, and the O₃/O₂ mixture was divided into two streams. One stream flowed through a wide-range ozone analyzer (BMT-964BT, OSTI Inc., 0 to 20 g/Nm³, ± 0.1 g/Nm³), aiming to quantitatively measure the ozone concentration in O₃/O₂ mixtures. The other stream was controlled by a mass flow controller (Alicat Scientific, Inc.) and then evenly mixed with the other four gases, N₂, NO, SO₂, and VOCs, which were controlled by mass flow controllers (Beijing Sevenstar Flow Co., Ltd.). A quartz tube with an inner diameter of 13 mm was placed in the tubular furnace, filled with 1 g of SCC catalyst in the middle. The reaction temperature was monitored by a K-type thermocouple. The outlet of the tubular furnace was connected to a wet scrubbing system, of which the liquid phase was the 3 L NaOH solution with a concentration of 0.125 mol/L, with the pH value adjusted to ~ 5.5 by adding phosphoric acid, and the liquid–gas ratio was set to 2.5 L/h. The Gaset Dx4000 exhaust gas analyzer was utilized to determine the concentrations of all components in the exhaust gas before and after the catalytic ozonation system and scrubbing system.

The conversion efficiencies of multi-VOCs/NO/SO₂ are calculated with eq 1 as follows

$$\eta_M = \frac{[M]_{in} - [M]_{out}}{[M]_{in}} \times 100\% \quad (1)$$

where η_M refers to the conversion efficiency of target pollutant M and M refers to one of the multipollutants, including acetone/benzene/toluene/*o*-xylene/NO/SO₂. $[M]_{in}$ means the initial concentration of the target pollutant M, and $[M]_{out}$ means the outlet concentration of the target pollutant M.

The selectivity of NO₂ is calculated with eq 2 as follows

$$\Phi_{NO_2} = \frac{[NO_2]_{out}}{[NO]_{in} - [NO]_{out}} \times 100\% \quad (2)$$

where Φ_{NO_2} refers to the selectivity of NO₂. $[NO_2]_{out}$ is the outlet concentration (ppm) of the NO₂. $[NO]_{in}$ is the initial concentration (ppm) of the NO. $[NO]_{out}$ is the outlet concentration (ppm) of NO.

2.4. Catalyst Activity On-Site Evaluation in Industrial Testing. The on-site industrial testing facility was built within a textile company located in Anhui province, China, as shown in Figure S2. The textile mill has 7 production lines, and the production process will generate waste gas containing organic pollutants. Some removal devices have been equipped but fail to meet the emission requirements due to the lower removal efficiency. The whole process includes exhaust gas collection, primary scrubbing, heat conversion, high-voltage electrostatic treatment, and secondary scrubbing, during which the flue gas temperature at the entrance of the primary spray tower is <150 °C. The components of the exhaust gas before the secondary scrubbing may include acetone, benzene, toluene, heptane, *o*-xylene, and butyl acetate. The flue gas for the reaction came from the exhaust gas of the textile mill before the primary scrubbing and before the secondary scrubbing. The comprehensive evaluation system comprised an adjustable ozone generator, a catalytic reactor, and measurement equipment. The ozone output from the ozone generator was adjustable, and the outlet flow was determined by a float flowmeter. The catalytic reactor utilized a previously prepared 2.5 kg SCC catalyst coupled with ozone to remove multiple VOCs in the exhaust gas. The measurement equipment was one exhaust gas analyzer (Gaset Dx4000), aiming to confirm the VOC compositions and concentrations in the exhaust gas before and after the catalytic ozonation process. The flow rate of exhaust gas was 17–25 N m³/h, and GHSV (gas hourly space velocity) was 680–1000 mL/(g·h).

The conversion efficiencies of multi-VOCs are also calculated with eq 3 as follows

$$\eta_V = \frac{[V]_{in} - [V]_{out}}{[V]_{in}} \times 100\% \quad (3)$$

where η_V refers to the conversion efficiency of target pollutant V and V refers to one of the multi-VOCs. $[V]_{in}$ means the initial concentration of the target pollutant V, and $[V]_{out}$ means the outlet concentration of the target pollutant V.

3. RESULTS AND DISCUSSION

3.1. Catalytic Activity Evaluation on a Laboratory Scale. The simultaneous removal of multi-VOCs (acetone/benzene/toluene/*o*-xylene) and NO/SO₂ by catalytic ozonation over the SCC catalyst was first carried out in the laboratory to evaluate the catalytic activity of the SCC catalyst. The effects of different parameters on multipollutant degradation processes, including ozone dosage, temperature, GHSV, and the existence of SO₂, were investigated by experimental catalytic activity evaluation, aiming to provide experimental data for further practical application in industry.

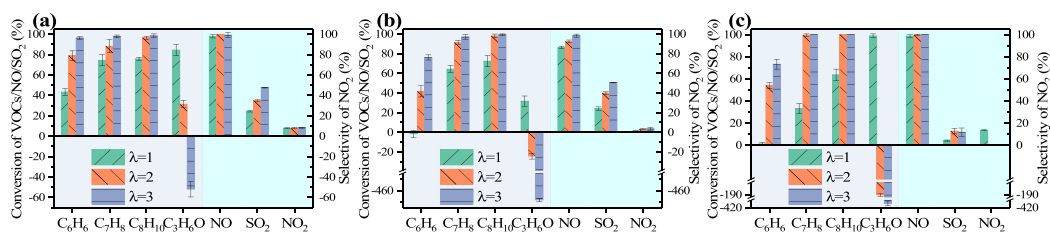


Figure 1. Effect of ozone dosage on the conversion efficiencies of multipollutants without the assistance of wet scrubbing under (a) 120 °C, 60000 mL/(g·h); (b) 50 °C, 60000 mL/(g·h); and (c) 50 °C, 240000 mL/(g·h).

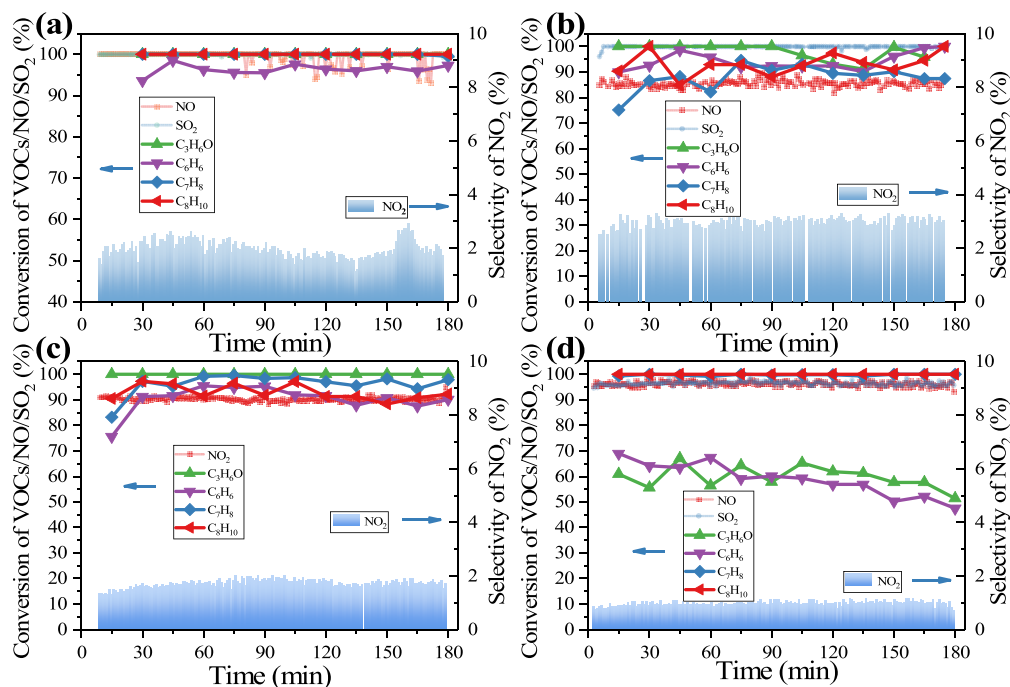


Figure 2. Conversion efficiencies of multipollutants with $\lambda = 3$ assisted by wet scrubbing under (a) 120 °C, 60000 mL/(g·h), with 200 ppm SO₂; (b) 50 °C, 60000 mL/(g·h), with 200 ppm SO₂; (c) 50 °C, 240000 mL/(g·h), without SO₂; and (d) 50 °C, 240000 mL/(g·h), with 200 ppm SO₂.

3.1.1. Effect of Ozone Dosage. In catalytic ozonation technology, the dosage of ozone, acting as a more potent oxidizer, plays a significant role in ensuring optimal activity performance. To achieve cost-effectiveness and prevent the unnecessary release of excess ozone, proper ozone dosage should be confirmed by an experimental test to provide the basis for parameter adjustment in practical industrial application. The excess ozone ratio (λ) was defined to describe the ozone dosage introduced into the catalytic ozonation system, referring to the ratio of the actual number of ozone moles to the theoretical number. The theoretical moles of ozone means the sum of the ozone moles for the equivalent ratio of four kinds of VOC oxidation reactions. The initial concentrations of multiple VOCs were 5 ppm acetone, 15 ppm benzene, 15 ppm toluene, and 15 ppm *o*-xylene. When the excess ozone ratio λ was 1, the ozone concentration was 283 ppm; when the excess ozone ratio λ was 2, the ozone concentration was adjusted to 567 ppm. An excess ozone ratio λ of 3 refers to an ozone concentration of 850 ppm. The activity measurement results of different excess ozone ratios λ are shown in Figure 1.

Figure 1 illustrates the degradation outcomes of multipollutants under different temperatures and different gas flows without the assistance of a wet scrubbing system, during which different dosages of ozone are introduced and λ varies from 1

to 3. It is obvious that among different reaction conditions, the trends in conversion efficiencies with the increase in λ are similar. Taking Figure 1(a) as an example, under 120 °C, when the λ increased from 1 to 3, the removal efficiency of NO was always maintained at around 100%, and there was little difference in NO₂ selectivity, generally less than 10%. This is corroborated by the research¹⁶ showing that when the O₃/NO molar ratio is >1, ozone can further oxidize NO₂ to N₂O₅. The removal efficiency of SO₂ also increased with the increase in ozone dosage, the maximum of which reached ~50% without a scrubbing system.

In Figure 1(a), focusing on the removal of multi-VOCs, a progressive enhancement in the removal efficiencies of aromatic VOCs corresponds to the gradual increase in the excess ozone ratio (λ) from 1 to 3. Notably, the removal efficiencies of toluene and *o*-xylene were less differentiating. The removal efficiencies of toluene and *o*-xylene were near 75% when λ was 1 and approached ~90% when λ increased to 2. When λ increased to 3, toluene and *o*-xylene could be completely removed. However, the removal efficiency of benzene was slightly lower than that of toluene and *o*-xylene, which was less than 50% when λ was 1. It increased to 80% when λ was 2 and was close to 96% when λ was 3. It can be seen that the SCC catalyst exhibited excellent activity for aromatic VOC removal, which may be related to the ratios of

$\text{Cr}^{6+}/\text{Cr}^{3+}$ and $\text{Co}^{2+}/\text{Co}^{3+}$ and abundant chemical-adsorbed oxygen of the catalyst,¹⁷ as shown in the XPS results below. In the process of the catalytic ozonation of VOCs, highly active oxygen atom species generated by ozone decomposition on the catalyst surface are also crucial for the oxidation of VOCs.^{18,19} The observed correlation indicates that a higher ozone concentration results in the generation of more active oxygen atoms generated by its decomposition, thereby contributing to the increase in the oxidation efficiencies of VOCs.

The removal of acetone is quite different from that of aromatic VOCs, as shown in Figure 1. For example, when λ increased from 1 to 3, in Figure 3(a), the removal efficiency of acetone gradually decreased from above 80% to ~30% and finally to a negative value, which showed that acetone was not completely degraded, even some of which was formed. According to the literature,²⁰ acetone is one of the intermediates in the decomposition processes of benzene, toluene, and *o*-xylene. When the ozone dosage gradually increases, more ozone preferentially reacts with aromatic VOCs, producing more intermediates, including acetone, resulting in a decline in the acetone removal efficiency and even turning it negative. This is consistent with the trends mentioned in the literature^{21–25} that aromatic VOCs are more easily destroyed than ketone VOCs. The difference in the conversion efficiencies of various VOCs is mainly due to the different affinities of the catalyst surface for different VOCs, which depend on the chemical structures,²¹ the competition of high-energy electrons and active radicals, and the interactions among various VOC molecules.^{5,22} In addition, the H_2O and CO_2 produced by the catalytic ozonation of aromatic VOCs²⁶ and the carbonaceous substances produced by incomplete oxidation^{23,27} will also inhibit the acetone conversion process. As discussed above, a series of factors could bring about the lower acetone removal efficiency compared to those of aromatic VOCs.⁵ This is highly consistent with the experimental phenomena reported in the literature.²³ In this article, three kinds of different aromatic VOCs and acetone were intended to be removed simultaneously, although the removal efficiency of acetone turned out to be even worse. Therefore, further improvement from assistance with the wet scrubbing system remains to be investigated.

3.1.2. Effects of Temperature, GHSV, and SO_2 . Aiming to improve the removal efficiency of acetone, characterized by its high solubility in water, as well as SO_2 and NO_2 , a scrubbing system was integrated with the catalytic ozonation setup to facilitate further removal processes.

In Figure 2(a), under the higher temperature of 120 °C, combined with the wet scrubbing system, the removal efficiency of NO was maintained above 95%, and the produced NO_2 that escaped was about 2 ppm, for which the selectivity was only 2%. With wet scrubbing, SO_2 was basically removed completely. For multi-VOCs, acetone, toluene, and *o*-xylene could be completely removed during the 3 h reaction process. The removal efficiency of benzene also fluctuated slightly in the range of 90–100%. This phenomenon was different from the results shown in Figure 1(a) without access to the scrubbing tower. With the incorporation of wet scrubbing, the removal efficiency of SO_2 was significantly increased, with NO_2 further absorbed into the liquid phase, and the removal efficiency of acetone was also significantly increased to nearly 100%. The results showed that the catalytic ozonation integrated with wet scrubbing technology could achieve the efficient and simultaneous removal of multipollutants, such as

VOCs, NO_x , and SO_2 , which provided an experimental basis for further industrial application.

Applicability in wide temperature ranges is also crucial for catalytic ozonation technology in industrial applications. In laboratory-scale experiments, the activity of the SCC catalyst on multipollutant simultaneous removal was also investigated under low temperatures. As can be seen from Figure 2(a),(b), the removal efficiencies of multiple pollutants decreased to varying degrees when the temperature was decreased to 50 °C. With the scrubbing system in Figure 2(b), SO_2 was basically removed completely, and the NO removal efficiency can also be maintained at 85%, with all VOC removal efficiencies maintained above 85%. Compared with activity measured under 120 °C in Figure 2(a), the activity of the SCC catalyst decreased slightly at 50 °C, but the conversion efficiency of 85% for multipollutant simultaneous removal could also be reached in combination with the scrubbing system, which also verified the applicability of the SCC catalyst at a lower temperature.

When the simulated flue gas flow was set as 1 L/min in Figure 2(a),(b), the calculated GHSV was 60000 mL/(g·h). In Figure 2(c),(d), the performance of the SCC catalyst in multipollutant simultaneous removal under a higher GHSV of 240000 mL/(g·h), with the simulated flue gas flow set as 4 L/min, was exhibited. In Figure 2(d), with a higher GHSV of 240000 mL/(g·h), at 50 °C, compared with the performance of the SCC catalyst under lower GHSV, the removal efficiencies of acetone and benzene were significantly reduced to ~50%, after being combined with the scrubbing system, which may be due to the more serious deactivation phenomenon of the SCC catalyst caused by larger flow of the simulated flue gas.

The presence of SO_2 is inevitable in the exhaust gas of various industries, the effect of which also should be investigated to evaluate the SO_2 -resistance ability of applied catalysts. The simultaneous removal efficiencies of multiple pollutants without SO_2 were measured to explore the effect of the SO_2 . It can be observed that in Figure 2(d) in the presence of SO_2 , the degradation efficiencies of acetone and benzene decreased to ~50%, while in Figure 2(c), without the presence of SO_2 , the removal efficiencies of all VOCs fluctuated above 90%, indicating that the presence of SO_2 will inhibit the catalytic ozonation process of VOCs, especially for acetone and benzene, which might be ascribed to partial poisoning of the SCC catalyst, caused by the accumulation of sulfates and sulfites produced on the catalyst surface, as verified by H_2 -TPR results in Section 3.3.3.^{5,8,9}

3.2. Application of Multi-VOCs' Simultaneous Removal in a Textile Mill.

3.2.1. Catalytic Activity Performance of the SCC Catalyst before Primary Scrubbing. Apart from the catalytic activity evaluation on a laboratory scale, the catalytic performance of prepared catalysts in industrial application is of high importance in verifying the realistic application feasibility of catalytic ozonation technology. Table S1 shows the main components and their maximum concentrations in the exhaust gas measured by a Gaset Dx4000 gas analyzer before primary scrubbing. Six kinds of main components in the exhaust gas before primary scrubbing could be observed from Table S1, which were, respectively, ethanol, acetone, carbonyl sulfur, trichloromethane, dichloroethane, and butyl acetate. Except ethanol, the initial maximum concentrations of the other five kinds of VOCs were all larger than 100 mg/Nm³, among which, that of dichloroethane was

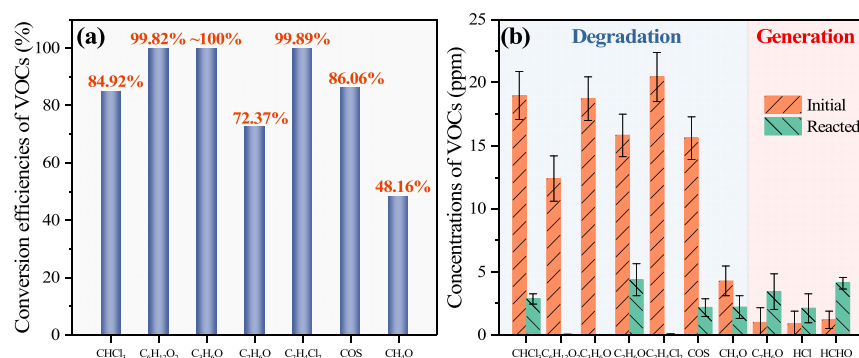


Figure 3. (a) Conversion efficiencies of multi-VOCs. (b) Concentration of multi-VOCs before and after the catalytic ozonation treatment.

up to 202.64 mg/Nm³, and initial concentrations of acetone and trichloromethane were also above 150 mg/Nm³.

During the activity evaluation, the ozone output was adjusted to 13 g/h and λ was 2. The removal efficiencies were calculated, as shown in Figure 3(a). When λ was 2, the removal efficiencies of acetone and butyl acetate were close to 100%, and the removal efficiencies of carbonyl sulfur, dichloroethane, and trichloromethane were also maintained at ~85%. The removal efficiency of ethanol was slightly lower, which can be dissolved in water; therefore, it is speculated that a higher removal efficiency can be achieved after the subsequent primary and secondary scrubbing.

When $\lambda = 2$, the changing trends in the concentrations of main VOC components and the small molecular VOCs generated are shown in Figure 3(b), divided into a degradation zone and a generation zone. The degradation components included the above six kinds of main VOCs pollutants with higher concentrations in Table S1 and methanol, but the removal efficiency of methanol was lower than those of the six major VOC pollutants, which might be ascribed to the fact that methanol was also one of the intermediate products during the multi-VOCs' degradation processes. The generated products mainly included hydrogen chloride, formaldehyde, and benzaldehyde, which were the main intermediate products produced in the catalytic ozonation process of multi-VOCs. The results were consistent with the conclusion in the literature¹¹ that the organic compounds mainly observed during acetone oxidation included formaldehyde, methanol, ketene, acetaldehyde, formic acid, and acetic acid, characterized and quantified by proton-transfer-reaction time-of-flight mass spectrometry (PTR-TOF-MS). The reaction mechanism of acetone oxidation in a dielectric barrier discharge (DBD) reactor was analyzed in detail:¹¹ first, acetone molecules were broken to form methyl radicals, acetyl groups, and H atoms, and then methyl radicals and acetyl groups were oxidized by O or OH radicals to form acetaldehyde, methanol, and other compounds. It might explain the lower removal efficiency of methanol in Figure 3(a). Acetaldehyde is the main intermediate produced by the oxidation of acetone, which will be decomposed and oxidized into other compounds, such as acetic acid and formaldehyde. This is consistent with the practical experimental results above, and formaldehyde in the generation zone in Figure 3(b) was the main generated product.

3.2.2. Catalytic Activity Performance of the SCC Catalysts before Secondary Scrubbing. The significance of the SCC catalyst in VOCs' simultaneous removal by ozonation assisted by wet scrubbing was investigated further. Before secondary

scrubbing, homogeneous ozonation and catalytic ozonation experiments were conducted in succession, compared, and recorded as cycle 2-1. The catalyst applied previously was utilized again for the second cycle of catalytic ozonation performance, recorded as cycle 2-2. The main components and their maximum concentrations in the exhaust gas before the secondary scrubbing are shown in Table S2, from which it was visible that the main components of the exhaust gas before the secondary scrubbing obtained from the two tests were consistent. There were four kinds of main components: phenol, *o*-xylene, heptane, and ethanol. It could be concluded by comparing Table S1 with Table S2 that there were large differences in the initial compositions of exhaust gas before primary and secondary scrubbing, such as the significant reduction of ethanol after primary scrubbing.

In the homogeneous ozonation process, without the SCC catalyst applied, the ozone dosage was adjusted to be increased from 13 to 30 g/h, and λ was 1–3. The removal efficiencies under different experimental conditions of homogeneous and catalytic ozonation processes are illustrated in Table 1. It is

Table 1. Removal Efficiencies of Different Components before Secondary Scrubbing (%)

Components		Phenol C ₆ H ₆ O	<i>o</i> -Xylene <i>o</i> -C ₈ H ₁₀	Heptane C ₇ H ₁₆
Homogeneous ozonation in cycle 2-1	$\lambda = 1$	50.09	50.05	22.83
	$\lambda = 2$	97.45	93.15	93.09
	$\lambda = 3$	99.07	98.52	100
Catalytic ozonation in cycle 2-2	$\lambda = 1$	56.51	2.96	19.89
	$\lambda = 2$	79.63	59.32	60.71
	$\lambda = 3$	98.21	98.56	87.50

shown in this table that, without the assistance of the SCC catalyst, increasing the ozone dosage, with λ increasing from 1 to 3, could also lead to higher removal efficiencies for the three main VOC pollutants. When λ was 2, the removal efficiencies of phenol, *o*-xylene, and heptane all reached above 93%, and under an λ of 3, the removal efficiencies of all VOC pollutants were close to 100%.

After the homogeneous ozonation process, the performance of ozonation coupled with the SCC catalyst was also explored, as shown in Figure 4, from which it could be concluded that, without catalytic assistance, VOCs with high molecular weight, including heptane, phenol, and xylene, were gradually degraded, but more small molecular VOCs such as methanol, formaldehyde, and formic acid were generated. Coupled with the SCC catalyst, with λ increasing from 1 to 3, small molecular VOCs were also gradually decomposed. Under $\lambda =$

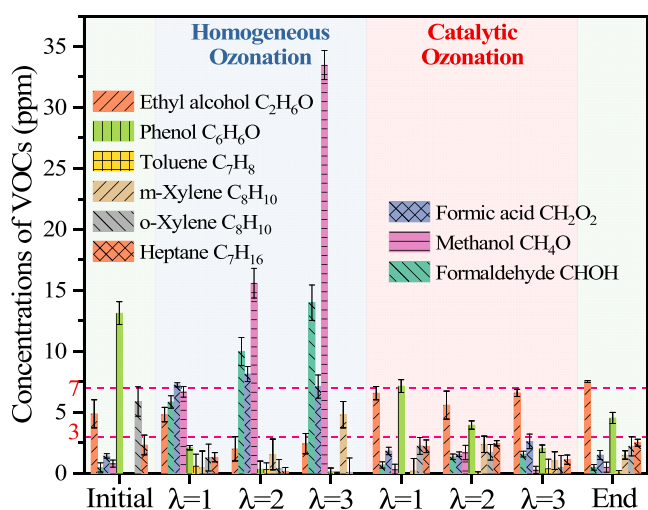


Figure 4. Concentrations of multi-VOCs in cycle 2-1.

3, the concentrations of major VOC pollutants could be degraded to below 3 ppm, as shown in Figure 4.

For industrial applications, the catalytic activity for recycling applied catalysts makes great sense for reducing costs and for simpler operation. In cycle 2-2, with the assistance of the SCC catalyst already applied in cycle 2-1, the removal efficiencies of multiple VOCs were clarified in Figure 5(a) and the efficiencies between the two cycles were compared in Figure 5(b), under different experimental conditions shown in Table 1. The trends were consistent with those of cycle 2-1, and the main VOC pollutants were still phenol, *o*-xylene, and heptane. By catalytic ozonation, small molecular VOCs such as methanol, formaldehyde, and formic acid were generated. When λ was 3, the removal efficiencies of phenol and *o*-xylene were 98%, and the removal efficiency of heptane was also above 87%, which verified the excellent catalytic activity of the SCC catalyst in the continuous industrial application of multi-VOCs' simultaneous removal.

Acetic acid and formic acid are important intermediates of acetone oxidation, according to the complete oxidation pathway of acetone on the 0.57 wt % CeO₂-0.05 wt % Pt/TiO₂ catalyst summarized in the literature.²⁸ And these are also the main intermediate products during the overall degradation reaction of the toluene/acetone binary mixture confirmed in the literature.²³ The intermediate products produced by incomplete oxidation from experimental results in this article

mainly included formic acid, methanol, and formaldehyde, consistent with the research results above.

3.3. Catalyst Characterization. **3.3.1. XRD Characterization.** Crystalline structures of the catalysts usually affect the catalytic performance of different catalysts in the process of oxidation and ozonation. The SCC catalyst prepared in this article was characterized by powder X-ray diffraction (XRD), and the XRD results are shown in Figure S3. As can be seen, the XRD curves of Cr1.5 and Co2.5-Cr1.5 catalysts prepared have strong diffraction peaks at 37.7, 45.8, and 66.8°, referring to the characteristic peaks of γ -Al₂O₃ (PDF no. 79-1558).²⁹ In addition, the XRD curve of the Cr1.5 catalyst also has several weak diffraction peaks of 35.1, 57.4, 43.3, and 25.5°, corresponding to the structure of Al_{1.92}Cr_{0.08}O₃ (PDF no. 87-0711). However, in the XRD curve of the Co2.5-Cr1.5 catalyst, the diffraction peak intensity of the Al₂O₃ structure is weakened, and the diffraction peaks of Cr₂O₃ and CoO_x can hardly be seen, indicating that CoO_x has good dispersion on the catalyst surface. After loading CoO_x, the relative intensities of all peaks gradually decrease, indicating the enhancement of the metal interaction.³⁰

3.3.2. ICP-OES Characterization. The actual loadings of Co and Cr in the prepared SCC catalysts were determined by ICP-OES (inductively coupled plasma optical emission spectroscopy). The characterization results are shown in Table S3. There is little difference between the actual loading and the designed one, and it can be confirmed that the mass fractions of Co and Cr are 2.5 and 1.5%, respectively.

The catalyst after the laboratory activity test was also characterized by ICP, and the results are shown in Table S3. It can be seen from the values in Table S3 that the mass fractions of Co and Cr in the catalyst decreased after the reaction, which is speculated to be related to catalyst deactivation. Along with the gradual reaction process, active Cr will be gradually lost, thus affecting the stability of chromium oxide catalyst activity,¹⁰ which is in agreement with the deactivation phenomenon in the previous laboratory acetone degradation work. The mass loss of the Co element may also be related to the removal reaction of VOCs.

3.3.3. Temperature-Programmed Performance. The O₂-TPD curves are commonly used to evaluate the desorption and mobility of oxygen,^{8,31} and those of fresh and spent SCC catalysts in this article are shown in Figure S4(a). Oxygen species can be divided into chemically desorbed oxygen O_α, surface lattice oxygen O_β, and bulk lattice oxygen O_γ, according to increasing desorption temperature.³¹ The desorption peaks

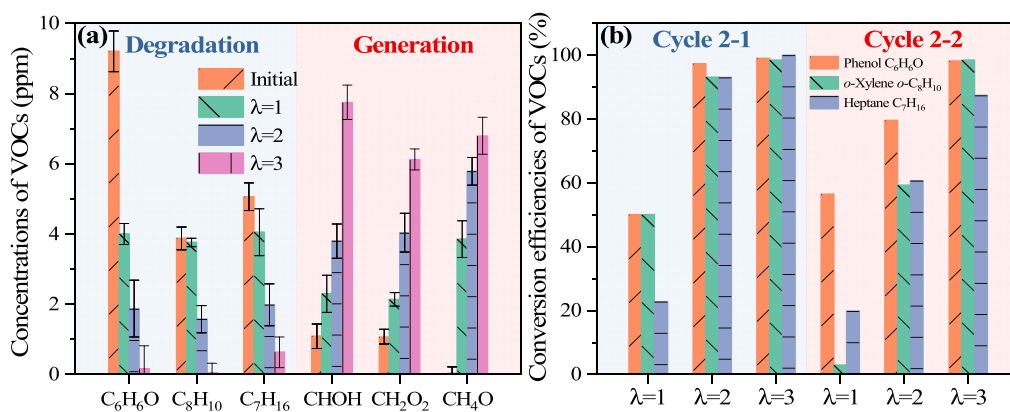


Figure 5. (a) Concentrations of multi-VOCs in cycle 2-2. (b) Comparison between conversion efficiencies of multi-VOCs in two reaction cycles.

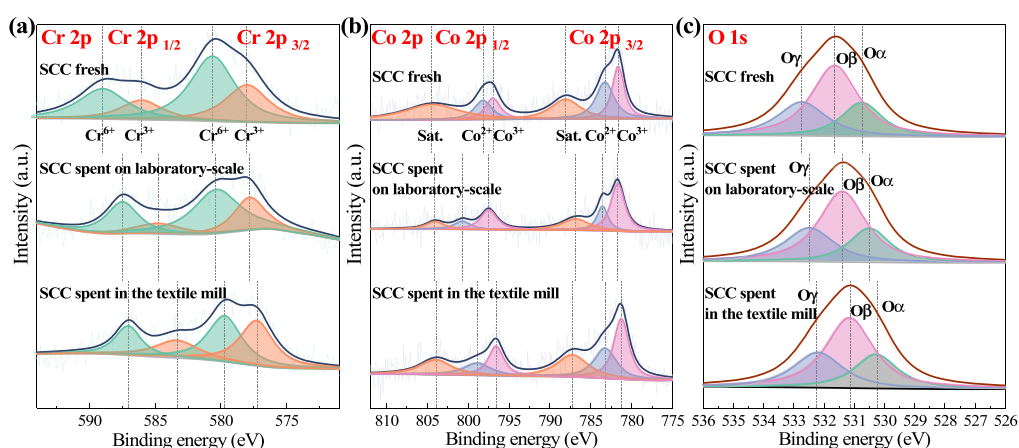


Figure 6. X-ray photoelectron spectra of different SCC catalysts: (a) Cr 2p, (b) Co 2p, and (c) O 1s.

Table 2. Distributions of Chromium, Cobalt, and Oxygen Species

catalysts	Cr distribution		Co distribution		O distribution			
	Cr ⁶⁺ /Cr	Cr ³⁺ /Cr	Co ³⁺ /Co	Co ²⁺ /Co	O _α	O _β	O _γ	O _β /O _α
SCC fresh	0.64	0.36	0.49	0.51	0.22	0.52	0.26	2.37
SCC spent on a laboratory scale	0.67	0.33	0.71	0.29	0.22	0.52	0.26	2.37
SCC spent in the textile mill	0.51	0.49	0.58	0.42	0.23	0.51	0.26	2.25

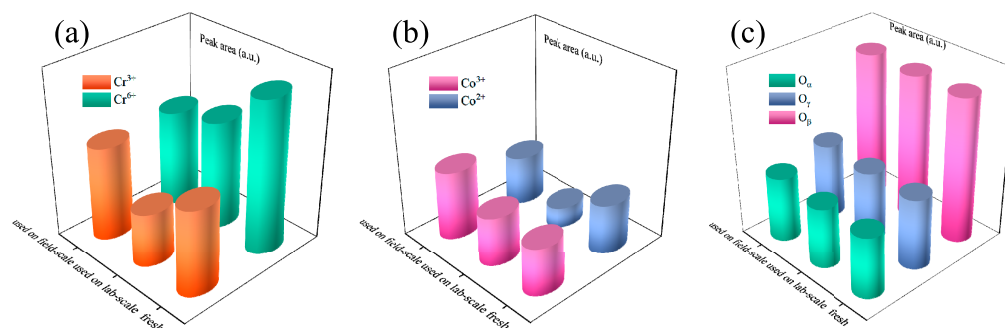


Figure 7. Valence distributions of different SCC catalysts: (a) Cr 2p, (b) Co 2p, and (c) O 1s.

below 300 °C illustrate the release of chemisorbed oxygen species.^{31,32} The peaks at 300–650 °C and above 700 °C refer to the desorption of surface oxygen and bulk lattice oxygen, respectively.^{8,31,32} The results in Figure S4(a) show that the fresh SCC catalyst possesses more active sites for O₂ desorption than the spent SCC catalyst applied for catalytic ozonation. Although there is no significant difference in the amount of chemisorbed oxygen in all SCC catalysts, the amount of surface oxygen species over the SCC catalyst decreased significantly after catalytic ozonation, which may affect the sustenance of SCC catalytic activity,^{8,32} leading to the deactivation observed from catalytic ozonation experimental results. The above conclusions are consistent with the analysis of O 1s spectra in XPS below.

In Figure S4(b) depicting the H₂-TPR curves, a broad reduction peak appears at 320 °C, corresponding to the reduction from Co²⁺ to Co⁰ or from Cr⁶⁺ to Cr³⁺.³³ This peak overlaps with a weaker peak at 395 °C, which indicates the reduction of highly dispersed Cr₂O₃.^{33,34} The H₂-TPR illustrates excellent reducibility of the fresh SCC catalyst at low temperatures, contributing to its high catalytic activity. It is acknowledged that with more H₂ consumption, the catalysts possess more oxygen vacancies and stronger reducibility, over

which adsorbed oxygen species could be desorbed more easily.^{8,35,36} Following application in the textile mill, all reduction peaks of the SCC catalyst become weaker, suggesting reduced H₂ consumption and weaker redox abilities. This phenomenon may be attributed to the decrease in the average oxidation valence,⁸ consistent with the XPS results shown in Figure 6. This might be due to the loss of active Cr⁶⁺ and Co²⁺, explaining the slight deactivation of the SCC catalyst continuously applied in the textile mill. From the H₂-TPR curve of the SCC catalyst applied on a laboratory scale, one sharper and stronger reduction peak shows up at higher temperature (530 °C), which is ascribed to the reduction of sulfates.³⁷ Because of the multiple pollutants' simultaneous removal in laboratory-scale experiments, including NO/SO₂ and multi-VOCs, the active metal oxides of the SCC catalyst are consumed and the surface becomes covered by metal sulfates or metal sulfides, causing the decrease in the reducibility, eventually leading to the deactivation of the SCC catalyst.

3.3.4. XPS. The redox ability of the catalysts depends on the different valences of the transition metals and their behavior in the catalytic reaction process also relies on the conversion of the different valence states, so it is of great significance to

analyze the change in the valence states of the elements on the catalyst surface.³⁷ The surface properties of different SCC catalysts before and after the ozonation reaction were obtained by XPS characterization, as shown in Figure 6. In Figure 6(a), the Cr 2p peak is divided into Cr 2p_{3/2} and Cr 2p_{1/2} parts,^{33,38} which are located at 577.1–580.3 and 583.2–588.7 eV, respectively. Cr 2p_{3/2} peaks could be deconvolved by XPS peak 41 software into different-valence peaks of Cr³⁺ and Cr⁶⁺, located at 577.7 and 580.3 eV, respectively.^{33,39} Analogously, the peaks of Cr 2p_{1/2} are deconvolved into two peaks at 585.7 and 588.7 eV, corresponding to Cr³⁺ and Cr⁶⁺, respectively.^{33,39}

According to the literature,^{33,34,40,41} the redox ability of Cr⁶⁺ is stronger than that of Cr³⁺, which is more conducive to the deep oxidation of VOCs. As can be seen from Table 2, the ratio of Cr⁶⁺/Cr in the fresh SCC catalyst reached 0.64, indicating the higher proportion of Cr⁶⁺, which is consistent with the excellent performance of the SCC catalysts in multi-VOC ozonation as described above, whether on the laboratory scale or in practical application.³³ In Figure 7, the content of Cr⁶⁺ in the fresh SCC catalyst is the highest, and those in spent SCC catalysts are reduced. This is consistent with the ICP results in Table S3, which may be due to the loss of the active Cr⁶⁺ during catalytic ozonation processes.⁵ As the reaction proceeded, the active Cr⁶⁺ in the SCC catalysts was gradually consumed, which changed the oxidation state, particle size, and dispersion of the catalyst and thus inhibited the activity of the SCC catalyst,⁵ also consistent with the deactivation phenomenon observed in our previous acetone degradation work.⁹

As shown in Figure 6(b), the XPS spectra of Co 2p include Co 2p_{3/2} and Co 2p_{1/2} peaks, respectively located at 781.1–783.5 and 796.4–800.6 eV and two corresponding satellite peaks, consistent with XPS results in the literature.^{42–44} After deconvolution, the two valence states Co³⁺ (781.3 and 796.6 eV) and Co²⁺ (782.9 and 797.8 eV) can be observed, mainly existing in the form of Co₂O₃ and Co(OH)₂, which is consistent with the XPS results in the literature.^{44–46} By calculating from the integration of the peak area, as Table 2 shows, on fresh SCC catalyst, the molar ratio of Co³⁺/(Co²⁺+Co³⁺) is 0.49, indicating that two Co ions with two different valences are in an equilibrium distribution on a fresh SCC catalyst.³⁷ A study⁴⁷ shows that the electron-transfer ability of Co²⁺ is higher than that of Co³⁺ in the process of catalytic ozonation, resulting in a higher conversion rate of ozone and a higher VOC conversion efficiency. As shown in Figure 7(b), the decrease in Co²⁺ content and the increase in Co³⁺ content are both visible after the catalytic reaction, which illustrates the participation of Co ions in the catalytic reaction process.^{43,48} It could be deduced that a part of Co²⁺ was transferred to Co³⁺ in the catalytic ozonation process of multipollutants. It is also reflected in Table 2 that the ratio Co³⁺/Co increased after the catalytic reaction, both on the laboratory scale and in practical application.

Concerning the O 1s spectra of the fresh SCC catalyst, it could be deconvolved into three peaks, of 530.4, 531.1, and 532.4 eV, which correspond to O_w, O_β, and O_γ, respectively. O_w located at ~530 eV, indicates the lattice oxygen, with sharper and stronger peak O_β referring to chemical-adsorbed oxygen, such as O⁻, O²⁻, O₂⁻, and O₂²⁻.^{8,38,49} O_γ demonstrates the presence of adsorbed H₂O/OH⁻ or carbonates.^{35,50} Besides, with higher mobility, O_β usually contributes as active sites for the adsorption of the gaseous O₂ into the oxygen

vacancy, which has a significant effect on the catalytic activity.^{8,51–53}

It could be noticed that the peak areas of O_β peaks in Figure 7(c) are similar, as well as O_β/O of different SCC catalysts in Table 2, although the O_β/O ratio of the SCC catalyst applied in the textile mill is a bit lower, which might be ascribed to its participation in the redox process of cobalt and chromium ions.^{43,46} This is consistent with the high activities and stabilities of those SCC catalysts, even those of applied ones. According to the literature,^{8,51,52} O_β chemically adsorbed oxygen, plays a dominant role in catalytic ozonation because of higher mobility causing more active surface oxygen vacancies as reaction sites. However, some shift to the lower binding energy of O_β could also be observed in spent SCC catalysts, meaning lower electron density and higher mobility after practical application.^{32,54}

The above XPS results show that rapid redox cycles of Cr³⁺/Cr⁶⁺ and Co²⁺/Co³⁺ and chemical-adsorbed oxygen all contribute to the catalytic performance of the SCC catalysts in the simultaneous removal of multipollutants.⁴³ The former pairs of Cr³⁺/Cr⁶⁺ and Co²⁺/Co³⁺ may provide donor–acceptor chemisorption sites for the reversible adsorption/desorption of oxygen on the SCC catalysts.⁴⁴

4. CONCLUSIONS

Different experimental parameters of multipollutant catalytic ozonation were investigated, including ozone dosage, temperature, and GHSV. With the increase in ozone dosage, removal efficiencies of most pollutants are improved, except that of acetone, which is one of the aromatic VOC degradation intermediates and is more difficult to degrade than BTX (benzene, toluene, and xylene). That is ascribed to the different structures, interactions among various VOC molecules, accumulation of CO₂/H₂O generated by complete oxidation, and carbonaceous substances from incomplete oxidation. Combined with the wet scrubbing method, by catalytic ozonation, conversion efficiencies could further be improved, achieving the simultaneous and efficient removal of multiple pollutants, including VOCs/NO/SO₂.

The lower temperature of 50 °C can cause inferior activity performance than that under the higher temperature of 120 °C, still with conversion efficiencies of multipollutants above 80%, verifying the applicability of low-temperature industrial conditions. Even for larger-flow flue gas, removal efficiencies of acetone and benzene decline to ~60% and those of others still stay above 90%, illustrating that the SCC catalyst coupled with ozone and wet scrubbing can adapt to multipollutant removal in flue gas within a certain range of gas flow or can apply to industrial conditions with less acetone and benzene, which could perform better without the existence of SO₂. The specific applications need to be adjusted according to the practical industrial conditions.

According to practical application in the textile mill, the main components of flue gas before the primary scrubbing are 6 different kinds of VOCs, of which most initial concentrations are larger than 100 mg/N m³. By catalytic ozonation technology, all removal efficiencies can achieve values >85%. The main intermediates are formaldehyde, hydrogen chloride, and benzaldehyde. The main components after the primary scrubbing are different from those before it, among which ethanol in particular decreased a lot by wet scrubbing. Without the SCC catalyst, the homogeneous ozonation reaction could also degrade the macromolecular VOCs with efficiencies above

90%, but micromolecular VOCs such as methanol, formaldehyde, and formic acid would still be generated, which are also the main intermediates of incomplete oxidation. The assistance of the SCC catalyst could contribute further to the decomposition of those micromolecular VOCs further.

The extraordinary activity of the SCC catalyst is ascribed to the good dispersion of CoO_x on the catalyst surface and the strong metal interaction. And the $\text{Cr}^{6+}/\text{Cr}^{3+}$ and $\text{Co}^{2+}/\text{Co}^{3+}$ rapid redox cycles and chemically adsorbed oxygen also contribute to its high catalytic activity and stability. It is also discovered that the deactivation of the SCC catalyst results from the decrease in Cr^{6+} and Co^{2+} as well as metal sulfates generated by the existence of SO_2 .

■ ASSOCIATED CONTENT

SI Supporting Information

The Supporting Information is available free of charge at <https://pubs.acs.org/doi/10.1021/acs.iecr.4c00675>.

Experimental set-up schemes on the laboratory scale and in a textile mill; XRD pattern of catalysts; temperature-programmed curves of different SCC catalysts; initial maximum concentrations of different components in exhaust gas before primary and secondary scrubbing; and ICP characterization results of catalysts (PDF)

■ AUTHOR INFORMATION

Corresponding Author

Zhihua Wang – State Key Laboratory of Clean Energy Utilization, Zhejiang University, Hangzhou 310027, P. R. China; orcid.org/0000-0002-7521-2900; Email: wangzh@zju.edu.cn

Authors

Peixi Liu – State Key Laboratory of Clean Energy Utilization, Zhejiang University, Hangzhou 310027, P. R. China; Centro de Química Estrutural, Instituto Superior Técnico, Universidade de Lisboa, Lisbon 1049-001, Portugal

Yiwei Zhang – State Key Laboratory of Clean Energy Utilization, Zhejiang University, Hangzhou 310027, P. R. China

Xiaojun Ma – Zhejiang Environmental Protection Group Co., Ltd., Hangzhou 310061, P. R. China

Chaoqun Xu – State Key Laboratory of Clean Energy Utilization, Zhejiang University, Hangzhou 310027, P. R. China

Yong He – State Key Laboratory of Clean Energy Utilization, Zhejiang University, Hangzhou 310027, P. R. China; orcid.org/0000-0002-7037-9007

Yanqun Zhu – State Key Laboratory of Clean Energy Utilization, Zhejiang University, Hangzhou 310027, P. R. China; orcid.org/0000-0002-0981-2078

Elisabete C. B. A. Alegria – Centro de Química Estrutural, Instituto Superior Técnico, Universidade de Lisboa, Lisbon 1049-001, Portugal; Departamento de Engenharia Química, Instituto Superior de Engenharia de Lisboa, Instituto Politécnico de Lisboa, Lisbon 1959-007, Portugal

Armando J. L. Pombeiro – Centro de Química Estrutural, Instituto Superior Técnico, Universidade de Lisboa, Lisbon 1049-001, Portugal; orcid.org/0000-0001-8323-888X

Complete contact information is available at: <https://pubs.acs.org/doi/10.1021/acs.iecr.4c00675>

Notes

The authors declare no competing financial interest.

■ ACKNOWLEDGMENTS

This work was supported by the “Pioneer” and “Leading Goose” R&D Program of Zhejiang [2023C03126]; by the National Natural Science Foundation of China [52125605] and the Fundamental Research Funds for the Central Universities [2022ZFJH04]; and in part by the Fundação para a Ciência e Tecnologia, Portugal [UIDB/00100/2020], [UIDP/00100/2020], [2022.02069.PTDC], and [LA/P/0056/2020] of Centro de Química Estrutural and by the Instituto Politécnico de Lisboa [IPL/IDI&CA2023/SMART-CAT_ISEL project].

■ REFERENCES

- (1) Qie, Z.; Zhang, Z.; Sun, F.; Wang, L.; Pi, X.; Gao, J.; Zhao, G. Effect of pore hierarchy and pore size on the combined adsorption of SO_2 and toluene in activated coke. *Fuel* **2019**, *257*, 116090.
- (2) Shi, Q.; Kang, D.; Wang, Y.; Zhang, X. Emission control of toluene in iron ore sintering using catalytic oxidation technology: A critical review. *Catalysts* **2023**, *13* (2), 429.
- (3) Lin, F.; Wang, Z.; Zhang, Z.; He, Y.; Zhu, Y.; Shao, J.; Yuan, D.; Chen, G.; Cen, K. Flue gas treatment with ozone oxidation: An overview on NO_x , organic pollutants, and mercury. *Chem. Eng. J.* **2020**, *382*, 123030.
- (4) Wu, X.; Yang, Y.; Gong, Y.; Deng, Z.; Wang, Y.; Wu, W.; Zheng, C.; Zhang, Y. Advances in air pollution control for key industries in China during the 13th five-year plan. *J. Environ. Sci.* **2023**, *123*, 446–459.
- (5) Liu, P.; Tang, H.; Shao, J.; He, Y.; Zhu, Y.; Alegria, E.; Wang, Z.; Pombeiro, A. J. L. Catalytic ozonation of multi-VOCs mixtures over Cr-based bimetallic oxides catalysts from simulated flue gas: Effects of $\text{NO}/\text{SO}_2/\text{H}_2\text{O}$. *Chemosphere* **2023**, *340*, 139851.
- (6) Jiang, K.; Yu, H.; Chen, L.; Fang, M.; Azzì, M.; Cottrell, A.; Li, K. An advanced, ammonia-based combined $\text{NO}_x/\text{SO}_x/\text{CO}_2$ emission control process towards a low-cost, clean coal technology. *Appl. Energy* **2020**, *260*, 114316.
- (7) Hutson, N. D.; Krzyzyska, R.; Srivastava, R. K. Simultaneous removal of SO_2 , NO_x , and Hg from coal flue gas using a NaClO_2 -enhanced wet scrubber. *Ind. Eng. Chem. Res.* **2008**, *47* (16), 5825–5831.
- (8) Shao, J.; Lin, F.; Wang, Z.; Liu, P.; Tang, H.; He, Y.; Cen, K. Low temperature catalytic ozonation of toluene in flue gas over Mn-based catalysts: Effect of support property and SO_2 /water vapor addition. *Appl. Catal., B* **2020**, *266*, 118662.
- (9) Liu, P.; Chen, L.; Tang, H.; Shao, J.; Lin, F.; He, Y.; Zhu, Y.; Wang, Z. Low temperature ozonation of acetone by transition metals derived catalysts: Activity and sulfur/water resistance. *Catalysts* **2022**, *12* (10), 1090.
- (10) Kang, D.; Bian, Y.; Shi, Q.; Wang, J.; Yuan, P.; Shen, B. A review of synergistic catalytic removal of nitrogen oxides and chlorobenzene from waste incinerators. *Catalysts* **2022**, *12* (11), 1360.
- (11) Zhang, C.; Wang, J.; Yang, S.; Liang, H.; Men, Y. Boosting total oxidation of acetone over spinel MCo_2O_4 ($\text{M} = \text{Co}, \text{Ni}, \text{Cu}$) hollow mesoporous spheres by cation-substituting effect. *J. Colloid Interface Sci.* **2019**, *539*, 65–75.
- (12) Wu, P.; Jin, X.; Qiu, Y.; Ye, D. Recent progress of thermocatalytic and photo/thermocatalytic oxidation for VOCs purification over manganese-based oxide catalysts. *Environ. Sci. Technol.* **2021**, *55* (8), 4268–4286.
- (13) Tomatis, M.; Xu, H.; He, J.; Zhang, X. Recent development of catalysts for removal of volatile organic compounds in flue gas by combustion: A review. *J. Chem.* **2016**, *2016*, 8324826.
- (14) Xi, Y.; Reed, C.; Lee, Y. K.; Oyama, S. T. Acetone oxidation using ozone on manganese oxide catalysts. *J. Phys. Chem. B* **2005**, *109* (37), 17587–17596.

- (15) Yu, S.; Niu, X.; Song, Z.; Huang, X.; Peng, Y.; Li, J. Improvement of Al_2O_3 on the multi-pollutant control performance of NO_x and chlorobenzene in vanadia-based catalysts. *Chemosphere* **2022**, *289*, 133156.
- (16) Asif, M.; Kim, W. Numerical study of NO_x abatement using ozone injection integrated with wet absorption. *Ozone-Sci. Eng.* **2014**, *36*, 472–484.
- (17) Zhao, Q.; Liu, Q.; Han, J.; Lu, S.; Su, Y.; Song, C.; Ji, N.; Lu, X.; Ma, D.; Cheung, O. The effect of cerium incorporation on the catalytic performance of cobalt and manganese containing layer double oxides for acetone oxidation. *J. Chem. Technol. Biotechnol.* **2019**, *94* (12), 3753–3762.
- (18) Reed, C.; Xi, Y.; Oyama, S. Distinguishing between reaction intermediates and spectators: A kinetic study of acetone oxidation using ozone on a silica-supported manganese oxide catalyst. *J. Catal.* **2005**, *235* (2), 378–392.
- (19) Konova, P.; Stoyanova, M.; Naydenov, A.; Christoskova, S.; Mehadjiev, D. Catalytic oxidation of VOCs and CO by ozone over alumina supported cobalt oxide. *Appl. Catal. A-Gen.* **2006**, *298*, 109–114.
- (20) Wang, Z.; Ma, P.; Zheng, K.; Wang, C.; Liu, Y.; Dai, H.; Wang, C.; Hsi, H.; Deng, J. Size effect, mutual inhibition and oxidation mechanism of the catalytic removal of a toluene and acetone mixture over TiO_2 nanosheet-supported Pt nanocatalysts. *Appl. Catal., B* **2020**, *274*, 118963.
- (21) Raju, B. R.; Reddy, E. L.; Karuppiiah, J.; Reddy, P. M. K.; Subrahmanyam, C. Catalytic non-thermal plasma reactor for the decomposition of a mixture of volatile organic compounds. *J. Chem. Sci.* **2013**, *125* (3), 673–678.
- (22) Beauchet, R.; Mijoin, J.; Batonneau-Gener, I.; Magnoux, P. Catalytic oxidation of VOCs on NaX zeolite: Mixture effect with isopropanol and *o*-xylene. *Appl. Catal., B* **2010**, *100* (1–2), 91–96.
- (23) Aghbolaghy, M.; Soltan, J.; Chen, N. Low Temperature catalytic oxidation of binary mixture of toluene and acetone in the presence of ozone. *Catal. Lett.* **2018**, *148* (11), 3431–3444.
- (24) Barakat, T.; Rooke, J. C.; Cousin, R.; Lamontier, J. F.; Giraudon, J. M.; Su, B. L.; Siffert, S. Investigation of the elimination of VOC mixtures over a Pd-loaded V-doped TiO_2 support. *New J. Chem.* **2014**, *38* (5), 2066–2074.
- (25) Burgos, N.; Paulis, M.; Mirari Antxustegi, M.; Montes, M. Deep oxidation of VOC mixtures with platinum supported on $\text{Al}_2\text{O}_3/\text{Al}$ monoliths. *Appl. Catal., B* **2002**, *38* (4), 251–258.
- (26) Auer, R.; Alifanti, M.; Delmon, B.; Thyron, F. Catalytic combustion of methane in the presence of organic and inorganic compounds over $\text{La}_{0.9}\text{Ce}_{0.1}\text{CoO}_3$ catalyst. *Appl. Catal., B* **2002**, *39*, 311–318.
- (27) Ghavami, M.; Soltan, J.; Chen, N. Enhancing catalytic ozonation of acetone and toluene in air using $\text{MnO}_x/\text{Al}_2\text{O}_3$ catalysts at room temperature. *Ind. Eng. Chem. Res.* **2021**, *60* (33), 12252–12264.
- (28) Wang, Z.; Li, S.; Xie, S.; Liu, Y.; Dai, H.; Guo, G.; Deng, J. Supported ultralow loading Pt catalysts with high H_2O -, CO_2 -, and SO_2 -resistance for acetone removal. *Appl. Catal. A-Gen.* **2019**, *579*, 106–115.
- (29) Long, L.; Zhao, J.; Yang, L.; Fu, M.; Wu, J.; Huang, B.; Ye, D. Room Temperature Catalytic Ozonation of Toluene over Transition Metal Oxides. *Chin. J. Catal.* **2011**, *32*, 904–916.
- (30) Shao, J. *Experimental and Mechanism Investigation on Catalytic Removal of NO_x and VOCs over Mn-Based Catalysts*; Zhejiang University, 2020.
- (31) Zhang, Z.; Xiang, L.; Lin, F.; Wang, Z.; Yan, B.; Chen, G. Catalytic deep degradation of Cl-VOCs with the assistance of ozone at low temperature over MnO_2 catalysts. *Chem. Eng. J.* **2021**, *426*, 130814.
- (32) Yang, H.; Du, J.; Wu, M.; Zhou, H.; Yi, X.; Zhan, J.; Liu, Y. Tin-modified $\alpha\text{-MnO}_2$ catalyst with high performance for benzene oxidation, ozone decomposition and particulate matter filtration. *Chem. Eng. J.* **2022**, *427*, 132075.
- (33) Su, J. *Experimental study on catalytic oxidation of DCM over HZSM-5 supported transition metal oxides*. Zhejiang University, 2016.
- (34) Yang, P.; Shi, Z.; Tao, F.; Yang, S.; Zhou, R. Synergistic performance between oxidizability and acidity/texture properties for 1,2-dichloroethane oxidation over $(\text{Ce,Cr})_x\text{O}_2/\text{zeolite}$ catalysts. *Chem. Eng. Sci.* **2015**, *134*, 340–347.
- (35) Wang, Z.; Liu, Y.; Yang, T.; Deng, J.; Xie, S.; Dai, H. Catalytic performance of cobalt oxide-supported gold-palladium nanocatalysts for the removal of toluene and *o*-xylene. *Chin. J. Catal.* **2017**, *38* (2), 207–216.
- (36) Bai, B.; Li, J.; Hao, J. 1D- MnO_2 , 2D- MnO_2 and 3D- MnO_2 for low-temperature oxidation of ethanol. *Appl. Catal., B* **2015**, *164*, 241–250.
- (37) Lin, F. *Basic characteristics study on NO_x deep removal in the flue gas by active molecules (ozone)-catalytic method*; Zhejiang University, 2018.
- (38) Li, X.; Cao, J.; Zhang, W. Stoichiometry of Cr(VI) immobilization using nanoscale zerovalent iron (NZVI): A study with high-resolution X-ray photoelectron spectroscopy (HR-XPS). *Ind. Eng. Chem. Res.* **2008**, *47* (7), 2131–2139.
- (39) Pradier, C. M.; Rodrigues, F.; Marcus, P.; Landau, M. V.; Kaliya, M. L.; Gutman, A.; Herskowitz, M. Supported chromia catalysts for oxidation of organic compounds: The state of chromia phase and catalytic performance. *Appl. Catal., B* **2000**, *27*, 73–85.
- (40) Lee, D. K.; Yoon, W. L. Ru-promoted $\text{CrO}_x/\text{Al}_2\text{O}_3$ catalyst for the low-temperature oxidative decomposition of trichloroethylene in air. *Catal. Lett.* **2002**, *81* (3), 247–252.
- (41) Ma, R.; Hu, P.; Jin, L.; Wang, Y.; Lu, J.; Luo, M. Characterization of $\text{CrO}_x/\text{Al}_2\text{O}_3$ catalysts for dichloromethane oxidation. *Catal. Today* **2011**, *175* (1), 598–602.
- (42) Cheng, M.; Zeng, G.; Huang, D.; Lai, C.; Liu, Y.; Zhang, C.; Wan, J.; Hu, L.; Zhou, C.; Xiong, W. Efficient degradation of sulfamethazine in simulated and real wastewater at slightly basic pH values using Co-SAM-SCS / H_2O_2 fenton-like system. *Water Res.* **2018**, *138*, 7–18.
- (43) Lu, S.; Wang, G.; Chen, S.; Yu, H.; Ye, F.; Quan, X. Heterogeneous activation of peroxymonosulfate by $\text{LaCo}_{1-x}\text{Cu}_x\text{O}_3$ perovskites for degradation of organic pollutants. *J. Hazard. Mater.* **2018**, *353*, 401–409.
- (44) Kaneti, Y. V.; Guo, Y.; Septiani, N. L. W.; Iqbal, M.; Jiang, X.; Takei, T.; Yuliarto, B.; Alothman, Z. A.; Golberg, D.; Yamauchi, Y. Self-templated fabrication of hierarchical hollow manganese-cobalt phosphide yolk-shell spheres for enhanced oxygen evolution reaction. *Chem. Eng. J.* **2021**, *405*, 126580.
- (45) Li, H.; Wan, J.; Ma, Y.; Wang, Y.; Chen, X.; Guan, Z. Degradation of refractory dibutyl phthalate by peroxymonosulfate activated with novel catalysts cobalt metal-organic frameworks: Mechanism, performance, and stability. *J. Hazard. Mater.* **2016**, *318*, 154–163.
- (46) Yang, W.; Chen, H.; Han, X.; Ding, S.; Shan, Y.; Liu, Y. Preparation of magnetic Co-Fe modified porous carbon from agricultural wastes by microwave and steam activation for mercury removal. *J. Hazard. Mater.* **2020**, *381*, 120981.
- (47) Aghbolaghy, M.; Ghavami, M.; Soltan, J.; Chen, N. Effect of active metal loading on catalyst structure and performance in room temperature oxidation of acetone by ozone. *J. Ind. Eng. Chem.* **2019**, *77*, 118–127.
- (48) Pang, Y.; Kong, L.; Chen, D.; Yuvaraja, G.; Mehmood, S. Facilely synthesized cobalt doped hydroxyapatite as hydroxyl promoted peroxymonosulfate activator for degradation of Rhodamine B. *J. Hazard. Mater.* **2020**, *384*, 121447.
- (49) Asami, K.; Hashimoto, K. An XPS study of the surfaces on Fe-Cr, Fe-Co and Fe-Ni alloys after mechanical polishing. *Corros. Sci.* **1984**, *24* (2), 83–97.
- (50) Shao, J.; Lin, F.; Li, Y.; Tang, H.; Wang, Z.; Liu, P.; Chen, G. Co-precipitation synthesized $\text{MnO}_x\text{-CeO}_2$ mixed oxides for NO oxidation and enhanced resistance to low concentration of SO_2 by metal addition. *Catalysts* **2019**, *9* (6), 519.

(51) Wang, X.; Liu, Y.; Zhang, T.; Luo, Y.; Lan, Z.; Zhang, K.; Zuo, J.; Jiang, L.; Wang, R. Geometrical-site-dependent catalytic activity of ordered mesoporous Co-based spinel for benzene oxidation: In situ DRIFTS study coupled with Raman and XAFS spectroscopy. *ACS Catal.* **2017**, *7* (3), 1626–1636.

(52) Sun, M.; Li, W.; Zhang, B.; Cheng, G.; Lan, B.; Ye, F.; Zheng, Y.; Cheng, X.; Yu, L. Enhanced catalytic performance by oxygen vacancy and active interface originated from facile reduction of OMS-2. *Chem. Eng. J.* **2018**, *331*, 626–635.

(53) Zhu, G.; Zhu, J.; Jiang, W.; Zhang, Z.; Wang, J.; Zhu, Y.; Zhang, Q. Surface oxygen vacancy induced α -MnO₂ nanofiber for highly efficient ozone elimination. *Appl. Catal., B* **2017**, *209*, 729–737.

(54) Lin, F.; Shao, J.; Tang, H.; Li, Y.; Wang, Z.; Chen, G.; Yuan, D.; Cen, K. Enhancement of NO oxidation activity and SO₂ resistance over LaMnO_{3+ δ} perovskites catalysts with metal substitution and acid treatment. *Appl. Surf. Sci.* **2019**, *479*, 234–246.